Adsorption versus grafting of poly(N-Isopropylacrylamide) in aqueous conditions on the surface of cellulose nanocrystals

Erwan Gicquel, Céline Martin, Laurent Heux, Bruno Jean, Julien Bras

Adsorption versus Grafting of Poly(N-Isopropylacrylamide) in aqueous conditions on the Surface of Cellulose Nanocrystals

Erwan GICQUEL[1], Céline MARTIN[1], Laurent HEUX[2], Bruno JEAN[2], Julien BRAS[1,3]

[1]*Univ. Grenoble Alpes, CNRS, Grenoble INP*, LGP2, F-38000 Grenoble, France*

[2]*Univ. Grenoble Alpes, CERMAV, F-38000 Grenoble, France ; CNRS, CERMAV, F-38000 Grenoble, France*

[3]*Institut Universitaire de Français, F-75000 Paris, France*

* Institute of Engineering Univ. Grenoble Alpes

_____

E-mail : julen.bras@lgp2.grenoble-inp.fr

ABSTRACT

This study proposes a grafting strategy of thermo-sensitive amine-terminated oligomers of Poly(N-Isopropylacrylamide) ($Pnipam_{2500}$) onto the surface of Cellulose Nanocrystals (CNCs). $Pnipam_{2500}$ grafting in aqueous condition via peptidic coupling was explored to obtain CNC hydrogel with thermo-reversible aggregation and new colloidal properties. A discussion between grafting vs adsorption /presence of the $Pnipam_{2500}$ is proposed. A large range of experimental techniques was used to investigate the properties of the CNC decorated with polymer and to confirm the grafting. Elemental analysis, infrared spectroscopy, solid state NMR and conductometric titration of washed CNC-g-$Pnipam_{2500}$ demonstrate that at least a part of $Pnipam_{2500}$ was covalently bonded with CNC. A thermo-reversible aggregation was observed by Dynamic Light Scattering experiments and thermo-sensitive behavior is observed by rheological experiments. For grafted polymer the viscosity increases from 0.008 to 40 Pa·s at low shear rate when the LCST is reached, whereas, in the case of polymer adsorption, the viscosity increases only from 0.002 to 0.3 Pa·s. This thermo-reversible, bio-based and biocompatible system paves the way for the design of injectable hydrogel and biomedical nanocomposite materials.

Keywords: Cellulose nanocrystals; Poly(N-Isopropylacrylamide); surface functionalization; thermo-sensitive

1. Introduction

The increasing interest to use biodegradable, renewable, non-toxic and sustainable material has led to the increasing use of nanoscale cellulose in advanced materials. Among such nanoscale cellulose, cellulose nanocrystals (CNCs) are obtained by acid hydrolysis and are rigid rod-shaped particles with dimensions ranging from 3 to 30 nm in cross-section and from 100 to 500 nm in length. Known since the 50's (Rånby, 1951), they exhibit several interesting properties including excellent mechanical strength, high aspect ratio, low density and an ability to self-organize into liquid crystalline phases (Habibi, 2014; Klemm et al., 2011; Moon et al., 2011; Revol et al., 1992). Besides, this treatment also introduces sulfate ester groups on the surface of CNC which induces a colloidal stability in aqueous media. Owing to their specific physical properties and high aspect ratio (depending on the source), CNC are used in several domains (Oksman et al., 2014) like environmentally friendly nanocomposites (Dufresne, 2013; Eichhorn et al., 2010; Siqueira et al., 2010a), biomedical applications (Camarero Espinosa et al., 2016; Domingues et al., 2014; Endes et al., 2016; Jorfi and Foster, 2015; Klemm et al., 2011; Lin and Dufresne, 2014; Naseri et al., 2016), coatings and printed electronics (Gicquel et al., 2017; Hoeng et al., 2016; Li et al., 2013), hydrogels and aerogels (De France et al., 2016, 2017; Eichhorn et al., 2010). Furthermore, CNCs are not only produced at laboratory scale but are now industrially available in high quantities (Chauve and Bras, 2014).

New properties can even be implemented to CNCs by modifying the numerous hydroxyl groups at their surface and several reviews focus on the chemical surface modification of CNC with molecule or polymers (Eyley and Thielemans, 2014; Habibi, 2014; Tang et al., 2017). Two main approaches can be used to covalently attach polymer chains on the surface of CNCs, the "grafting-from" or the "grafting-to" methods. The "grafting-from" allows highest grafting polymers length chains on CNCs surfaces and highest grafted polymer diversity. For the grafting from approach, the surface is first functionalized with an initiator monolayer. Then, the polymerization is carried out on the surface-initiated, resulting on the growth of the polymer brush directly from the surface (Alosmanov et al., 2017; Dong and Roman, 2007; Follain et al., 2010; Kan et al., 2013; Wu et al., 2015; Zoppe et al., 2010). However, the "grafting-from" method induces the presence of free homopolymers and generally uses toxic solvents or reagents.

In the “grafting-onto” strategy, a greener process can be tested. Presynthesized and well characterized polymer chains are reacted with cellulose hydroxyl groups or surface carboxylate groups generated by TEMPO oxidation. Nonetheless, steric hindrance can prevent optimal grafting and limit the grafts surface density. As examples of the “grafting-onto” process, Araki et al. and Kloser et al. respectively grafted epoxy-terminated polyethylene glycol (PEG) and polyethylene oxide (PEO) on CNC to create sterically stabilized system (Araki et al., 2001; Kloser and Gray, 2010; Mangalam et al., 2009).

In this study, the “grafting-onto” strategy is used. The aim is to create a covalent amide bond between a primary amine-terminated thermo-sensitive polymer and carboxylated CNC as shown in **Figure 1**. In the literature, this approach has been successfully applied by coauthors to the grafting of copolymers of ethylene oxide and propylene oxide , referred to as Jeffamine polyetheramines (Huntsman Corporation) on TEMPO oxidized CNC (Azzam et al., 2010, 2016). First, CNC are oxidized and then reacted with amine-terminated polymers using a carbodiimide as amidation agent. Such reactions can be performed in an organic solvent or in aqueous media (Azzam et al., 2010, 2016) but requires long reaction times and washing steps. As reported in the literature, the realization of stimuli-sensitive CNC complex represents an interesting way to design smart hydrogel and materials, in particular in the field biomedical applications (Jorfi and Foster, 2015; Naseri et al., 2016).

In this work, we have focused on the peptidic grafting of one of the most common thermo-sensitive polymer Poly(N-Isopropylacrylamide) also called PNIPAM. This polymer exhibits a lower critical solution temperature (LCST) at 32°C. Below the LCST, the polymer chains are in good solvent conditions and adopt a swollen coil conformation with highly hydrated chains. Above the LCST, the polymer becomes hydrophobic and turns into a collapsed globule (Lai et al., 2013; Pelton, 2010; Plunkett et al., 2006; Schild, 1992). PNIPAM shows a LCST close to physiological temperature whatever almost irrespective of its molecular weight (Okahata et al., 1986), and has a huge potential in biomedical applications (Alosmanov et al., 2017; Chen et al., 2014; Hebeish et al., 2014). Its bio-compatibility and non-toxicity were discussed in a recent review by Lanzalaco et al. (Lanzalaco and Armelin, 2017) and detailed in vivo experiments with cartilage formation (Cho et al., 2004), ocular integration (Cao et al., 2007; Lima et al., 2016), subcutaneous tissues (Ohya et al., 2004), cell sheets (Lin et al., 2012) or drug release (Das et al., 2015).

In the literature, the “grafting-from” method has mainly been used to graft this thermo-sensitive chains (Alosmanov et al., 2017; Hemraz et al., 2014; Zoppe et al., 2010, 2011; Zubik et al., 2017). Zoppe and co-workers (Zoppe et al., 2010, 2011) grafted PNIPAM brushes from CNC via SET-LRP, in which they control exactly the density and the length of brushes depending on the ratio of initiator and molecular ratio of NiPAAm monomer. However, such strategy needs toxic solvent and to the best of our knowledge, no previous works propose “grafting-onto” of PNIPAM on CNCs.

Meanwhile, more and more studies prove the possibility of high adsorption of poly-electrolyte or oligomers on the surface of CNC using various techniques like QCM or SPR (Reid et al, 2017; Benselfelt et al, 2016). In some case, it seems even possible to have irreversible adsorption and no desorption is observed in spite of multiple washing steps.

In this paper, we compare the surface functionalization of CNCs with amine-terminated thermosensitive PNIPAM chains using either simple adsorption or peptidic coupling. The new systems are then characterized by conductometric titration, infrared spectroscopy, solid state NMR and elemental analysis. Dynamic light scattering (DLS) and transmission electron microscopy (TEM) are used to describe the structural modification of the nanoparticles.

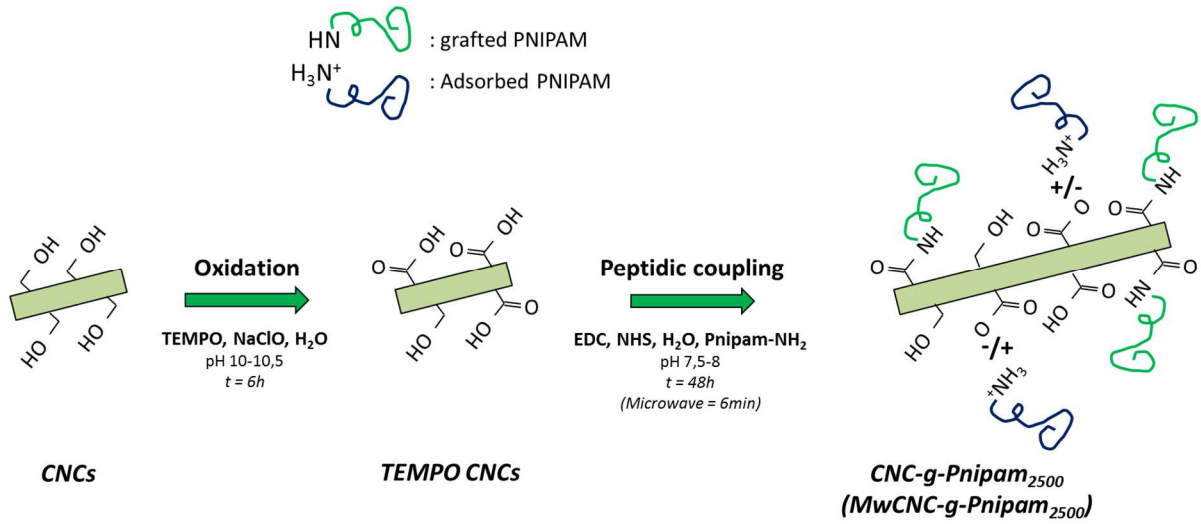

***Figure 1**: Schematic representation of chemical modification on CNCs presents in this work*

2. Materials and Methods

2.1. Materials

Colloidal suspension of ~12 wt.% Commercial Cellulose Nanocrystals (CNCs) was purchased from UMaine process Development Center (University of Maine, USA). They have been produced from wood pulp using sulfuric acid hydrolysis process and have been never freeze-dried. The dry matter was measured using a moisture analyzer (Ohaus® MB-35, Sigma-Aldrich, USA). Poly(N-Isopropylacrylamide) with amine terminated was purchased from Sigma-Aldrich (USA). The molecular weight is about 2500 $g \cdot mol^{-1}$, and the LCST is close to 32°C. For the TEMPO oxidation, following chemicals are purchased from Sigma-Aldrich: 2,2,6,6-Tetramethyl-1-piperidinyloxy (TEMPO, 2564-83-2), Sodium hypochlorite (NaClO, 12 wt.%, 7681-52-9) and Sodium bromide (NaBr, 7647-15-6). For the peptidic grafting, chemicals are purchased from Sigma-Aldrich: N-(3-Dimethylaminopropyl)-N'-ethylcarbodiimide hydrochloride (EDC, 25952-53-8) and N-Hydroxysuccinimide (NHS, 6066-82-6). Other chemicals were purchased from Sigma-Aldrich. Distilled water was used for all experiments.

2.2. Carboxylation of cellulose nanocrystals by TEMPO oxidation

CNCs were subjected to TEMPO-mediation oxidation using a previously reported procedure (Habibi et al., 2006). 11 g of CNC were dispersed in 730mL of distilled water. Then, this suspension was exposed to an ultrasonic dispersive energy of 5 kJ per gram of dry CNC using a 250 Watt sonication probe (Sonifier S-250A, Branson, USA) at 50% of maximum energy during 15 minutes in this case. To prevent burning of CNC during the dispersion, the suspension was placed in a crystallizer full of ice. TEMPO (323 mg, 2.07 mmol) and NaBr (3.564 mg, 34.61 mmol) were dissolved in 250mL of deionized water by magnetic stirring and slowly added to the CNC suspension. Then, 66 g (0.12M) of NaClO suspension was added dropwise to the suspension to start the oxidation. The mixture was stirred for 3 h at room temperature. The pH condition of the suspension was maintained between 10 and 10.5 by addition of sodium hydroxide solution (NaOH) at 0.5M during the reaction. Reaction was then quenched by the addition of ethanol (40 ml), the suspension color turned from yellow to white. The resulting CNC were washed with hydrochloric acid (HCl) at 0.5M, to decrease the pH to 1-2, at least three times by centrifugation (10 000 rpm, 30 min). After the last

centrifugation, the oxidized CNC were re-dispersed in distilled water using the minimum volume to recover all CNC. This suspension was dialyzed against distilled water at least one week until a neutral pH was obtained (membrane 6-8 kDa). TEMPO CNCs were stored in the fridge at constant neutral pH to allow the CNC to be in their carboxylate form.

2.3. Polymer grafting by peptidic coupling in water

Grafting of amine-terminated $PNIPAM_{2500}$ on TEMPO CNCs was performed by peptidic coupling in water according to protocol of Bulpitt and Aeschlimann (Bulpitt and Aeschlimann, 1999). The reaction was performed at ambient temperature, and started with a ~1 wt.% TEMPO CNCs suspension, N_{COOH} is the mole of carboxyl unit measured by conductometry. This suspension was exposed to an ultrasonic dispersive energy using a 250 Watt sonication probe (Sonifier S-250A, Branson, USA) at 50% of maximum energy during 80 seconds per dry grams of CNC to remove any aggregates. The pH was adjusted to 4.5 (CNC-COOH configuration) with 0.5M HCl. Then, 2mL of EDC solution was added to the suspension (N_{EDC}: mol per carboxyl group) and stirred during 30 min. Then, 2mL of NHS solution was added (N_{NHS}: mol per carboxyl group) and stirred during 30 min. The pH was then adjusted to 7.5-8.0 before the addition of 10mL of an aqueous suspension containing PNIPAM-NH_2 (N_P: mol per carboxyl group). In accordance with the protocol of Azzam et al. (Azzam et al., 2010), all results were obtained with $N_{EDC} = N_{NHS} = N_P = 4 \times N_{COOH}$. The reaction lasted 48 h at room temperature under stirring while maintaining the pH at 7.5-8.0 by addition of 0.5M NaOH or 0.5M HCl. The reaction was quenched by the decreasing of the pH at 1-2 by addition of 0.5M HCl and the resulting suspension was dialyzed against distilled water to remove excess of reagents at least seven days with exchange of water regularly until neutral pH is obtained. $PNIPAM_{2500}$ grafted CNC will be referred to as CNC-g-$Pnipam_{2500}$.

2.4. Conductometric and pH-metric titrations: Carboxyl content

The carboxyl content of oxidized CNC and grafted CNC were determined by conductometric titration coupled with pH-metric titration. About 15 mg of CNC was suspended in 200 mL of distilled water and treated by ultrasonic bath for 5min to remove gas and increase the dispersion. The pH of the suspension is adjusted to acidic condition (pH = 3) with 0.1 M HCl to replace the sodium counter-ions by protons. The suspension was then titrated with 0.2 mL increment of 0.01 M NaOH. The titration curves exhibit two turns: the first one

corresponds to the NaOH neutralization of the strong acid due to the excess of HCl, and then follows by the neutralization of the weak acid related to the carboxyl content.

Degree of Oxidation (DO) of oxidized CNC is the number of primary hydroxyl groups that have been oxidized into carboxyl groups per AnhydroGlucose Unit (AGU). It was calculated according to the following **Equation 1** from Da Silva Perez et al. (Da Silva Perez et al., 2003):

$$\mathrm{DO} = \frac{162 \times C \times (V_{eq2} - V_{eq1})}{m - 36 \times C \times (V_{eq2} - V_{eq1})} \qquad (1)$$

Where 162 (g·mol^{-1}) corresponds to the molar mass of an AGU, C (mol·L^{-1}) is the exact concentration of the NaOH solution, m (g) is the weight of the oven-dried sample, 36 in g·mol^{-1} corresponds to the difference between the molecular weight of an AGU (162 g·mol^{-1}) and that of the sodium salt of a glucuronic acid moiety (198 g·mol^{-1}), and V_{eq1} and V_{eq2} are the equivalent volumes of NaOH on the bends during the titration. To minimize errors, titrations were reproduced at least three times and an average value was used for the discussion.

Equation 2 gives the calculation of the oxidation charge concentration (X_{ox}), in µmol·g^{-1}:

$$\mathrm{X}_{ox} = \frac{C \times (V_{eq2} - V_{eq1})}{m} \qquad (2)$$

Where C (mol·L^{-1}), m (g), V_{eq1} and V_{eq2} are the same as previously.

After grafting by peptidic coupling, a part of the carboxyl groups is consumed in the reaction with the amine-terminated polymer. A new oxidation rate X_{res} (in µmol·g^{-1}), corresponded to the residual carboxyl content, was calculated after conductometric titration as given by the following **Equation 3**:

$$\mathrm{X}_{res} = \frac{C \times (V_{eq4} - V_{eq3})}{w} \qquad (3)$$

Where C (mol·L^{-1}) is the exact concentration of the NaOH solution, w (g) is the pure dry CNC weight in total samples weight of the oven-dried sample and V_{eq3} and V_{eq4} are the equivalent volumes of NaOH on the post-grafting titration.

Finally, the percentage of carboxyl groups which has been substituted ($\%\mathrm{COOH}_{\mathrm{grafted}}$) was calculated according to the equation **Equation 4**, and represents the peptidic coupling yield:

$$\%\mathrm{COOH}_{\mathrm{grafted}} = \frac{\mathrm{X}_{ox} - \mathrm{X}_{res}}{\mathrm{X}_{ox}} \times 100 \qquad (4)$$

2.5. Fourier transform infra-red spectroscopy (FTIR)

Infrared spectra of oxidized CNC and grafted CNC were performed using a Perkin-Elmer spectrum 65 (PerkinElmer, USA). Prior to avoid the superposition of the carbonyl band with the one of the water, CNC suspensions were acidified to pH 3. Samples were dried during 2 h in an oven at 80°C and reduced in powder form prior to analysis. KBr pellets containing 1 wt.% solid cellulose sample were prepared. At least spectra of two samples (to check the reproducibility) per type of CNC were recorded in transmission mode with 16 scans in the 400-4000 cm^{-1} wavenumber range.

2.6. Elemental analysis (EA)

Elemental analysis was carried out by the Analysis science institute of the "centre national de la recherche scientifique", Lyon, France. The Carbon, Hydrogen, Oxygen, Sulfur and Nitrogen contents for CNC, TEMPO CNC, CNC-g-$Pnipam_{2500}$ and MwCNC-g-$Pnipam_{2500}$ were measured independently. The obtained results from elemental analysis were used to determine the Degree of Oxidation after TEMPO oxidation (DO_{EA}) (**Equation 5)**:

$$DO_{EA} = \frac{72.07 - \%C1 \times 162.14}{\%C1 \times 35.93} \qquad (5)$$

Where %C1 corresponds to the relative carbon content in oxidized sample and 72.07, 162.14, 35.93 are respectively the molecular weight of carbon in AGU, molecular weight of an AGU, the difference between the molecular weight of an AGU and an oxidized AGU with sodium salt.

2.7. Solid-State NMR

NMR experiments were performed with a Bruker Avance DSX 400 MHz spectrometer operating at 100.6 MHz for ^{13}C, using the combination of cross-polarization, high-power proton decoupling and magic angle spinning (CP/MAS) methods. The spinning speed was set at 12 kHz. The ^{1}H radio frequency field strength was set to give a 90° pulse duration at 2.5µs.

The ^{13}C radio frequency field strength was obtained by matching the Hartman-Hahn conditions at 60 kHz. Recording at least 2000 transients with contact time and recycle delay, respectively, of 2 ms and 2 s represented standard conditions. The acquisition time was set at 30 ms and the sweep width at 29400 Hz. The position and width of the lines were maintained constant throughout a series of samples. The area corresponding to the integration of the C_1 signal was used as an internal standard and set to one.

2.8. Transmission Electron Microscopy (TEM)

Drops of about 0.001 wt.% of CNC suspension were deposited onto glow-discharged carbon-coated TEM grids. After 2 minutes, the liquid in excess was absorbed with filter paper, and prior to drying, a drop of Urany-Less (Delta Microscopies, France) was deposited on the specimen. Then, after 2 minutes, the solution in excess was adsorbed and the grid was dried under room temperature. The sampling was observed using a Philips CM200 (FEI, USA) operating at 200 kV.

This protocol was adapted to account for the LCST of the grafted thermo-sensitive polymer (~32°C). In a first case, TEM specimens were prepared at room temperature. In a second case, TEM specimens were prepared with CNC-g-$Pnipam_{2500}$ suspension and Urany-Less solution both preheated at 50°C.

2.9. Dynamic light scattering (DLS)

DLS measurements were performed on Malvern Nano ZS instrument (Malvern instruments, United Kingdom). Samples were diluted in deionized water at 10^{-2} wt.% and the conductivity was adjusted to 500 $\mu S \cdot cm^{-1}$ by addition of NaCl solution. All measurements were made at a well-controlled (± 0.05°C) temperature at a backscattering detection angle of 173°. Non-negative least squares analysis (NNLS) was performed to achieve the intensity size distribution (corresponding to hydrodynamic diameter z*) from the analysis of the correlation function on the Malvern DTS software. For each samples, the final data in this paper represent an average of at least 3 acquisitions with 10 measurements.

2.10. Atomic Forces Microscopy (AFM)

CNCs were imaged using AFM (Dimension icon®, Bruker, USA). All suspensions were previously diluted to 10^{-4} wt.% and a drop of 0.2 mL was deposited onto a freshly cleaved

mica plate. Samples were dried overnight at room conditions. The samples were characterized in tapping mode using a silica coated cantilever (OTESPA® 300 kHz - 42 N/m, Bruker, USA). Scans of 10x10 μm^2 and 3.3x3.3 μm^2 were performed to analyze the dimensions of CNC. At least 4 images per sample were obtained. In order to extract the length and height dimensions, measurements of about 200 particles were performed by using the ImageJ software to obtain a representative average size.

3. Results and Discussion

3.1. Grafting of amine terminated Pnipam$_{2500}$ onto TEMPO CNCs

Aqueous commercial CNC suspensions were previously carboxylated using TEMPO oxidation process. By conductometric titration (**Figure S1a – Support information**) and **Equation 1**, a degree of surface oxidation DO of 0.25 (mol/mol of anhydroglucose unit) and an oxidation rate X_{ox} of 1450 (µmol·g^{-1}) were obtained.

Aqueous TEMPO CNCs were then grafted with amine terminated Pnipam$_{2500}$ via peptidic coupling. **Figure S1b (Support information)** reports conductometric titration. After calculation with **Equation 2** and **Equation 3**, the residual carboxyl content (X_{res}) is 1010 (µmol·g^{-1}) and the percentage of carboxyl groups which has been substituted by amine groups ($\%COOH_{grafted}$) is 30 %.

Nevertheless, these results are indirect proof of the grafting and would be similar in case of adsorption. FTIR spectroscopy and Elemental Analysis were performed to confirm the presence of the polymer chains onto the CNC. **Figure 2** shows FTIR spectra of (**Figure 2a**) regular CNC, (**Figure 2b**) TEMPO CNCs, (**Figure 2c**) TEMPO CNCs mixed with Pnipam$_{2500}$ and (**Figure 2d**) CNC-g-Pnipam$_{2500}$. All samples have been extensively washed before any characterization using dialysis.

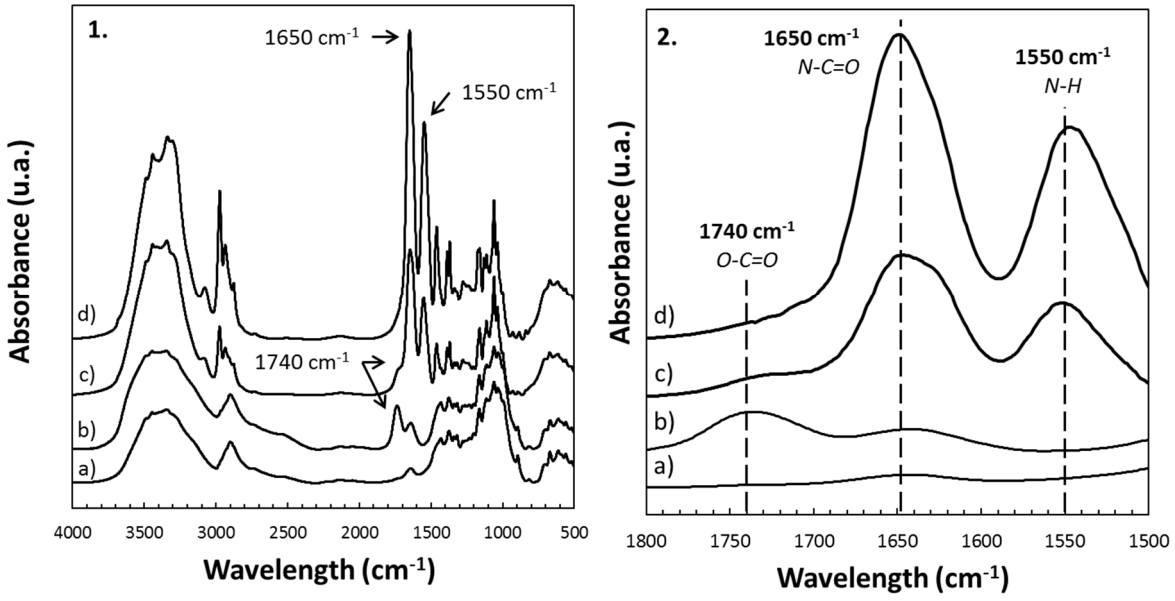

***Figure 2**: 1. Infrared spectra of a) sulfated commercial CNCs, b) TEMPO CNCs c) TEMPO CNCs mixed with $Pnipam_{2500}$ and d) $Pnipam_{2500}$ grafted onto CNCs: CNC-g-$Pnipam_{2500}$. Each spectrum is normalized at 1110 cm^{-1}. 2. Infrared Spectra zoom on characteristic peaks.*

Clear changes occur in each steps of the chemical modification. By comparing to the commercial CNCs, the spectra of the TEMPO CNCs exhibits a high absorption band at 1740 cm^{-1}. This peak is characteristic to the acidic form of the carboxylic acid function (COOH), which validated the oxidation of CNCs. In the case of a peptidic grafting, peaks characteristic of the amide bonding appear in two absorption bands. Unfortunately, in our case such amide bonds are also present in the polymer and cannot prove the grafting but mainly the presence or not of the polymer. The first band at 1650 cm^{-1} can be attributed to the amide bond (amide I absorption band) but also to the residual water adsorbs on the cellulose (or polymer). Furthermore, at 1550 cm^{-1}, another absorption peak characteristic of the N-H bond exists (called amide II band). On the **Figure 2c**, referring to $Pnipam_{2500}$ only mixed with TEMPO CNCs without coupling agent and following similar washing steps, the two characteristic peaks of amine are present (1650 and 1550 cm^{-1}). They prove the presence of $Pnipam_{2500}$ in the suspension of CNCs even without grafting and after the washing steps. This result was surprising and we have first checked the efficiency of our washing procedure. By dialysis of pure $Pnipam_{2500}$ during 7 days, we have checked that most of the polymer (ab. 80-85%) pass through the membrane and is eliminated during the dialysis. The 15-20% still present seems to be non-solubilized / aggregated polymer or impurities nanoparticles (like catalyst) present in this commercial grades, as proved by some DLS measurement showing some aggregates or impurities of about 200nm dimensions. So as most of the $Pnipam_{2500}$ is eliminated, the **Figure 2c** confirms the presence of oligomer in the suspension. We can suppose this due to the aggregate and to the physically adsorbed oligomer onto the CNC surface. This adsorption might be due to the hydrogen bonds and has been investigated more in details in recent study (Gicquel, 2017).

However, the presence of a small peak at 1740 cm^{-1} (e.g. COOH characteristic pic) indicates that still some carboxylic ends are available after adsorption and washing. In the case of the grafted sample (**Figure 2d)**, the two characteristic peaks of the amine bond are present (1650 and 1550 cm^{-1}). Even if it is not quantitative proof, the intensities of these peaks are largely superior to those one of $Pnipam_{2500}$ adsorbed on CNCs. Besides, as previously said PNIPAM-NH_2 contains N-H bonds in the repeating NIPAM monomer. The molecular weight

~2500 g·mol^{-1} corresponds to ~22 time of monomer (~22 amine groups) and one amine on the termination. So, with a superior intensity compared to **Figure 2c**, more Pnipam$_{2500}$ are present on the CNCs' surface which might be due to a different polymer configuration on the surface. In this case, the grafting efficiency is also revealed thanks to the disappearance of the 1740 cm^{-1} peak which probably reveals the consumption of CNC's carboxyl groups in the reaction with the amine-terminated polymers. This disappearance might be due also to overlapping with peak at 1650cm^{-1}. Probably one part of Pnipam$_{2500}$ is adsorbed and one part is grafted in this case but it is difficult to separate the amount of grafted and adsorbed polymer on CNCs.

So this FTIR analyses proves the presence of Pnipam$_{2500}$ into oxidized CNCs suspension. Such oligomer stays in the suspension in spite of washing steps but also that when grafting is performed a higher quantity seems present and all carboxylic group disappears.

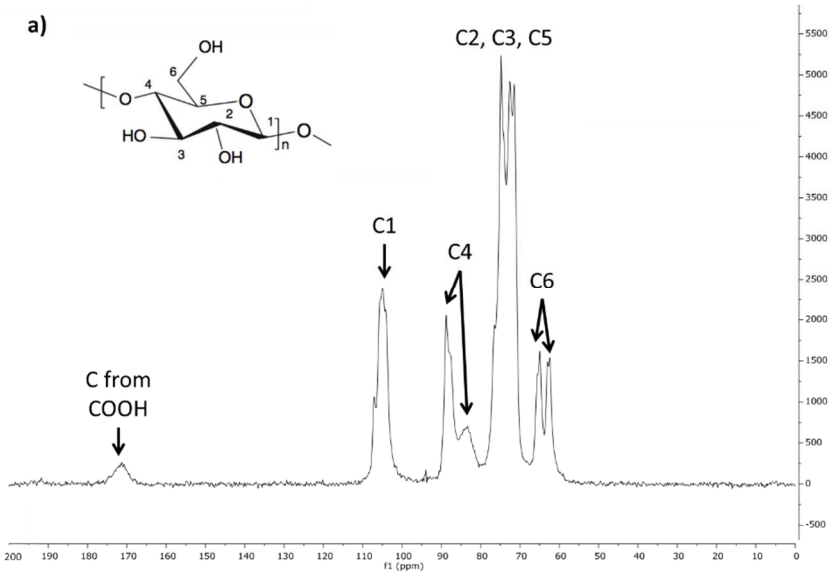

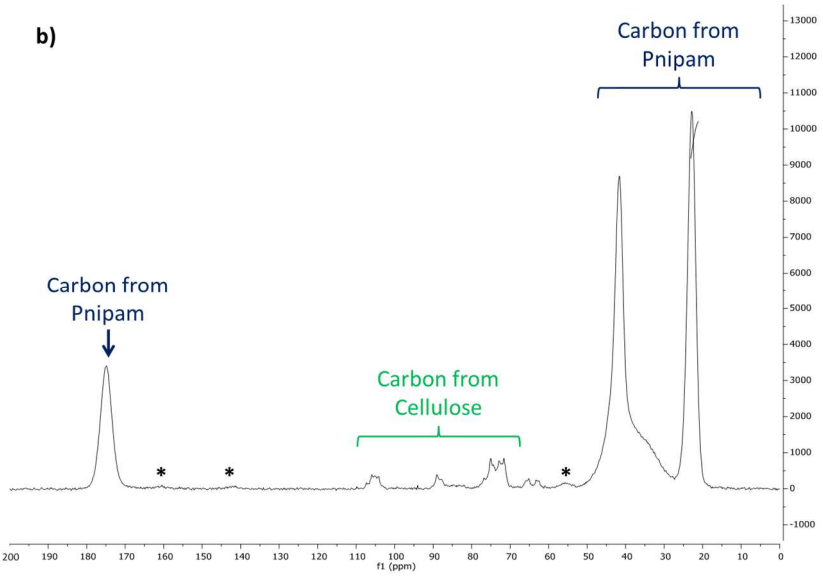

***Figure 3**: ^{13}C Solid-state NMR spectra of A. TEMPO CNCs and B. CNC-g-Pnipam$_{250}$. Stars (*) correspond to the spinning side band of Pnipam$_{2500}$ at 10 kHz (results not shown). Insert figure shows chemical structure related to C_1-C_6 of cellulose.*

Figure 3 shows the ^{13}C solid-state NMR of TEMPO CNCs and CNC-g-Pnipam$_{2500}$. In the case of TEMPO CNCs (**Figure 3a**), carbon contribution of the cellulose were clearly identified (Atalla and VanderHart, 1999; Montanari et al., 2005). The region between 60 and 70 ppm correspond to the C_6 carbon of the AGU, and between 70 and 80 ppm to the carbon contribution of the C_2, C_3 and C_5. C_4 contribution is the region between 83 and 88 ppm. The C_1 carbon appears at 105 ppm. The area corresponding to the integration of the C_1 signal was used as an internal standard and set to one. The contribution of the carboxyl group is located at 174 ppm (Montanari et al., 2005). The **Figure 3b** represents the NMR spectra after the grafting of Pnipam$_{2500}$ on CNCs (after dialysis washing steps). On this spectrum, the contribution of the carbon from the polymer is very high related to the internal standard on C_1 (from 20 to 36 times the integration of the C_1 signal). The peptidic grafting creates a new link between carbon and nitrogen (i.e. a new amide). As already said, this link is also present inside the NIPAM monomer of the polymer chain, so it is difficult to separate the contribution of the carbon amide occurring after the grafting from the carbon amide in polymer contribution. The disappearance of the peak at 174 ppm (related to COOH) replaced by a strong peak at 176 ppm (related to -CONH-) could be due to the grafting but also to solid "dilution" due to the presence of Pnipam$_{2500}$ and high amount of amide bounds. The **Figure 3b** reveals indeed the presence in huge amount of PNIPAM on the CNCs surface after several washing steps. These values are in accordance with a presence of Pnipam$_{2500}$ on

TEMPO CNCs surface, but cannot confirm if it is grafted or adsorbed. A comparison with only mixed $Pnipam_{2500}$ would not help due to this dilution but could give us more quantitative information. For such quantitative data, we have preferred using elemental analysis.

3.2. Quantitative analysis of $Pnipam_{2500}$ onto CNCs

Further evidence of the grafting of $Pnipam_{2500}$ from CNCs was supported by the elemental analysis of extensively washed CNC and used to quantify the amount of polymer present on the surface. **Table 1** shows the experimental atomic composition (C, H, N, O and S) of CNCs, TEMPO CNCs, CNC-g-$Pnipam_{2500}$ and CNCs mixed with $Pnipam_{2500}$.

Table 1*: Atomic composition determined by Elemental Analysis (standard deviation is considered to be related to equipment at 0.1 % for each value).*

	Experimental values					*Corrected values*	
	% C	% H	% N	% O	% S	% C	%O
CNCs	40.2	6.0	< 0.1	49.7	0.9	44.44	49.37
TEMPO CNCs	37.0	5.9	< 0.1	52.2	0.8	40.91	51.80
CNC-g-$Pnipam_{2500}$	53.8	8.9	8.9	24.3	0.3	59.50	27.11
TEMPO CNCs + $Pnipam_{2500}$	53.9	8.8	9.1	24.2	0.2	59.69	24.04

In the case of pure cellulose, theoretical values of the weight fraction of carbon are 44.44% and 49.37% for oxygen, and theoretical ratio of oxygen-to-carbon is close to 1.11. Therefore, experimental value presents a ratio about 1.24 for CNC. It is well known that the difference between the theoretical and the experimental values in the case of the carbon content is probably due to sulfate content, the impurities present in the sample and experimental error. To incorporate this difference, the experimental values reported in **Table 1** are corrected with the product between the experimental value obtained for a given material and the ratio of the theoretical to experimental value for non-grafted nanoparticles. This strategy has already been used to determine the degree of substitution (Missoum et al., 2012; Siqueira et al., 2010b).

In the case of TEMPO CNCs, the DO_{EA} calculated from the **Equation 5** gives an oxidation rate of about 0.38 which is close and in the same range than conductometry titration value (i.e. DO = 0.25) if we consider the standard deviation of E.A. From these results, it is possible

to estimate the surface density of the carboxyl content and to calculate the maximum amount possible of polymers which can be grafted. After a TEMPO oxidation, carboxylic groups are mainly on the surface of CNCs (Isogai et al., 2011). With a DO of about 0.25 and assuming that the surface of an AGU is 1 nm^2, it corresponds to a density ~25 COOH every 100 nm^2, assuming that most of oxidation occurs at the surface of CNC. CNC dimensions a x b x c are 150 x 10 x 10 nm^3 (**Table 2**). As the surface of CNC is 6000 nm^2, 1500 COOH ends are available on the surface. The maximum grafting molecule will be with 1500 polymer chains per CNC. Referring to the conductometric titration, ~30 % carboxyl groups were substituted by amine groups. It corresponds to ~450 polymer chains grafted on the surface of CNCs.

The presence of a high amount of nitrogen content in the CNC-g-$Pnipam_{2500}$, extensively washed confirms that $Pnipam_{2500}$ is still present after grafting on TEMPO CNCs. This value is equivalent to the quantity of $Pnipam_{2500}$ of 5 wt.% using ratio of %C/%N with following **Equation 6** and **7**.

$$\%C = \frac{[(1 - \%Pnipam_{2500}) \times M_C \times 6] + [\%Pnipam_{2500} \times (M_C \times 134)]}{M_{tot}} \quad (6)$$

$$\%N = \frac{\%Pnipam_{2500} \times M_N \times 23}{M_{tot}} \quad (7)$$

Where $(1 - \%Pnipam_{2500})$, M_C, 6, $\%Pnipam_{2500}$, 134, M_N, 23 and M_{tot} are respectively the CNC mass, carbon molecular weight, number of carbon in AGU, mass of $Pnipam_{2500}$, number of carbon in $Pnipam_{2500}$, Nitrogen molecular weight, number of nitrogen in $Pnipam_{2500}$ and total mass. To evaluate the number of CNCs in a suspension, the density of cellulose (1.59) and dimension of CNC (a x b x c = 150 x 10 x 10 nm^3) were used.

Based on the presence of ~4 E^{16} CNCs in 0.95 g of suspension (1g – 5% of $Pnipam_{2500}$) and ~1200 E^{16} $Pnipam_{2500}$ chains in 0.05 g of suspension, this value of 5 wt.% means ~300 polymer chains on the surface of TEMPO CNCs. This value shows that all the COOH have not been grafted. But it is difficult to say if it is grafted or adsorbed. Indeed, unfortunately similar amount of $Pnipam_{2500}$ is present when only adsorption and washing occurs.

If we consider only adsorption, the surface of adsorbed polymer chains should be characterized by a mushroom regime, in which they do not interact together, in the case of

moderate polymer densities. The size of the polymer is in the order of the gyration radius, which is 1.5 nm, given by $R_g = 0.022 \times {M_w}^{0.54}$ (Kubota et al., 1990) where M_w is the polymer molecular weight, *i.e.* 2500 g·mol^{-1}. To be in mushroom regime, each polymer needs to be at a distance higher than twice time the R_g. The CNC size a x b x c are 150 x 10 x 10 nm^3, equivalent to an area about 6000 nm^2. The surface occupied by a polymer is 7 nm^2 ($\pi \times {R_g}^2$), so on a CNC the maximum of adsorbed polymer is ~860 polymer chains. This value is in the range of grafting calculation. So in both case, adsorption and grafting, similar amount of polymer chain can be present on CNC surface.

As a conclusion, it is difficult to have a direct proof of the grafting vs adsorption/presence with techniques we have used. Our assumption is that similar amount of $Pnipam_{2500}$ is at the surface of CNC but in the case of adsorbed polymer, all polymer is present as aggregate in the suspension or at the surface whereas when it is grafted, one part is grafted on the surface and another part is adsorbed or present as aggregate.

Indirect methods have then been performed to check if we have a difference between grafted and adsorbed system. Furthermore, the elemental analysis gave us an idea of the ratio of $Pnipam_{2500}$ and CNC. This has been confirmed by weight measurement of suspensions. Indeed, after grafting, all samples are washed directly with dialysis, so we are sure that CNCs stays (does not pass through dialysis membrane). So, knowing the initial CNCs mass and just by measuring the final mass, we can calculate the quantity of $Pnipam_{2500}$ which is still present (adsorbed or grafted or both). In our case this weight measurement gives a ratio of 25% of CNC and 75% of PNIPAM after adsorption and after grafting. This value will be considered in DLS characterization (**Figure 4**).

3.3. Thermosensitive behavior of CNCs decorated with Pnipam$_{2500}$

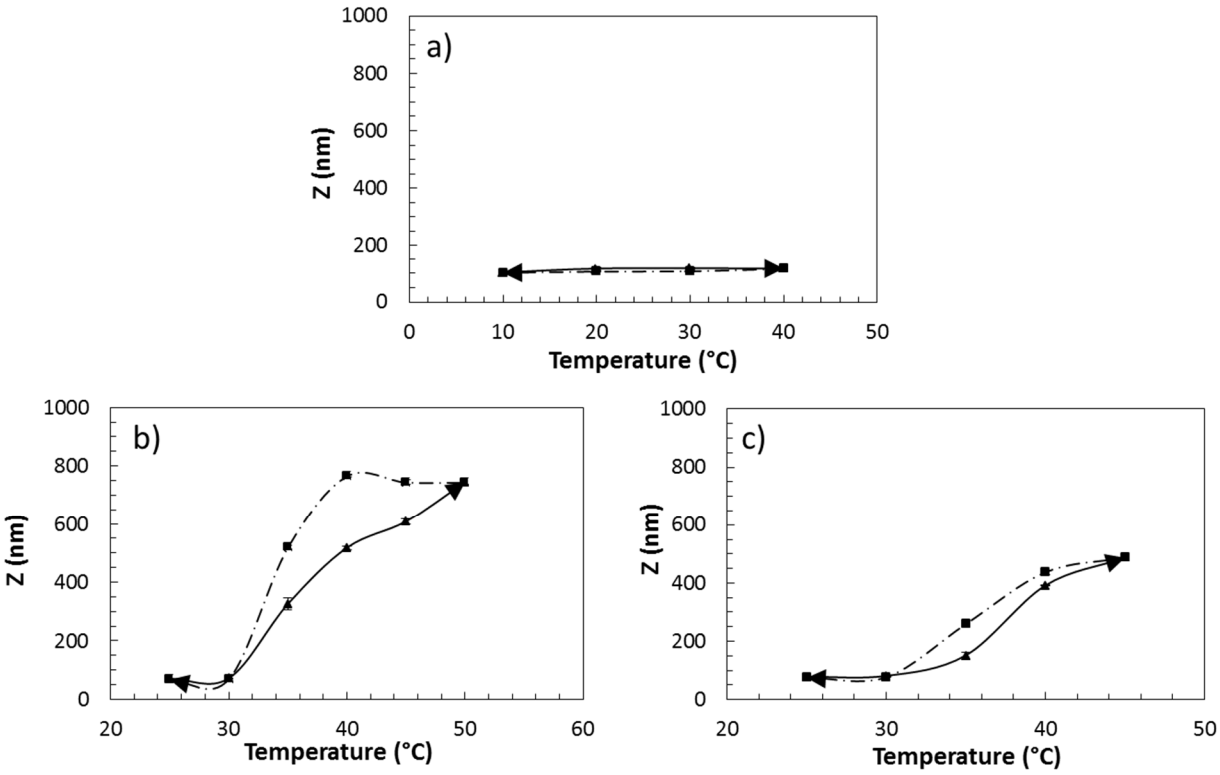

***Figure 4**: DLS curve for (a) TEMPO CNCs at 0.1 wt.%, (b) CNC-g-Pnipam$_{2500}$ at 0.1 wt.% (ratio estimated at 25% CNC and 75% Pnipam$_{2500}$) and (c) TEMPO CNCs + Pnipam$_{2500}$ (ratio at 25% TEMPO CNCs and 75% Pnipam$_{2500}$). Full line: temperature increases and dot line: Temperature decreases.*

In **Figure 4**, the hydrodynamic diameter of CNC-g-Pnipam$_{2500}$ and TEMPO CNCs + Pnipam$_{2500}$ suspension and CNCs raw materials were measured as function of temperature. For TEMPO CNCs (**Figure 4a**), temperature has no clear influence on the size of the particles. Referring to the literature (Fujishige et al., 1989; Wu, 1998), PNIPAM shows sensitivity to the temperature. In works of Kubota (Fujishige et al., 1989; Kubota et al., 1990; Senff and Richtering, 1999; Wu, 1998) and Wu (Wang and Wu, 1999; Wu, 1998), under the LCST (~34°C), PNIPAM polymer presents coil conformation with hydrodynamic diameter about 100 nm. In our case the measurement of DLS was difficult due to the presence of impurities (catalyst nanoparticles or other) detected with an initial DLS value of 500nm which is not possible for a so short oligomer. Then above the LCST, the polymer turns in globule conformation and presents a hydrodynamic diameter about 20 nm. For the grafting sample CNC-g-Pnipam$_{2500}$ (**Figure 4b**), under the LCST the hydrodynamic diameter is low and constant (close to the CNC size as it is a short oligomer). After 30°C, an increase in size was observed (750 nm), probably due to aggregates formation. When the sample is cooling back to 20°C, the hydrodynamic diameter decreases and, at T < 30°C the system recovers a low

438 and constant value similar to the one measured during the heating process. This
439 phenomenon is considered reversible, even if a 5°C hysteresis is observed. This result is very
440 positive and confirms indirectly that at least a part of CNC is grafted mainly when it is
441 compared with only adsorbed $Pnipam_{2500}$ (**Figure 4c**). In this case, the aggregation is limited
442 compared to grafted molecule, and the maximum collapse system size is close to 480 nm (vs
443 610 nm for the grafted CNC at same Temperature). The difference is even higher when
444 temperature decrease, i.e. 480 for adsorbed and 750nm for grafted CNC. Nonetheless, the
445 thermo-reversible behavior is similar in the case of grafted or adsorbed $Pnipam_{2500}$. So the
446 thermo-stimuli properties of CNC-g-$Pnipam_{2500}$ and TEMPO CNCs + $Pnipam_{2500}$ are different.
447 This confirms indirectly that we don't have only presence or adsorption in the first case.

448 The grafting of $Pnipam_{2500}$ polymer chain on the surface of CNCs gives a thermo-reversible
449 behavior to the suspension, as proved by the thermo-reversible aggregation in DLS data. The
450 behavior of a PNIPAM polymer was previously explained in detail (Lai et al., 2013). In this
451 study, when the temperature is below the LCST of $Pnipam_{2500}$, grafted chains are under good
452 solvent conditions. Steric repulsion forces between particles are maximal, and dispersion
453 with individual objects appears. For temperature higher than the LCST, the polymer is in
454 poor solvent condition in water, resulting in individual collapsed and CNC-g-$Pnipam_{2500}$ are
455 aggregated together. This process is reversible and generates a hysteresis effect. Similar
456 behavior was observed with another thermosensitive polymer grafted onto CNC (Azzam et al
457 2016).

3.4. CNCs and Pnipam$_{2500}$ grafted onto CNCs (CNC-g-Pnipam$_{2500}$) characterization

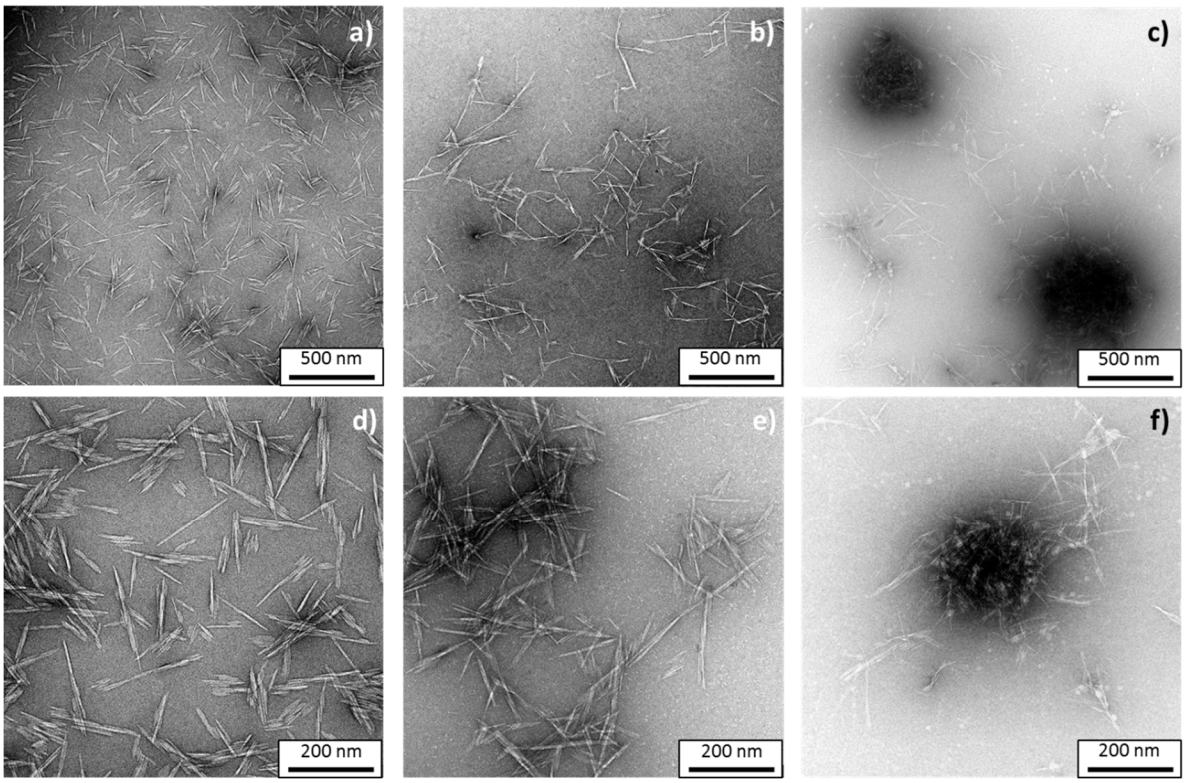

***Figure 5**: TEM images of a)-d) Cellulose Nanocrystals (CNCs) before any treatment and b)-e) CNC-g-Pnipam$_{2500}$ deposed on TEM grid at 20°C and c)-f) CNC-g-Pnipam$_{2500}$ deposed at 50°C. Pictures are representatives of each sample.*

As confirmed in **Figure 5a** and **5d**, CNC have a rod-like shape. Size measurements on TEM images show an average length of 150 ± 30 nm and a section of 10 ± 5 nm. These values are comparable with the literature data (Habibi et al., 2010).

***Table 2**: Physical and chemical properties of CNCs from university of Maine.*

Properties		**Tools**	**Value**	**S.D.**
Morphology	Length (nm)	*AFM & TEM*	150	(30)
	Thickness (nm)		10	(5)
	Aspect ratio		15	-
Chemical	Sulfur content (µmol/g$_{CNC}$)	*EA*	305	(15)
Physicochemical	Surface charge density (e/nm²)	*Calculation based on EA & TEM*	0.46	(0.02)

In details in **Table 2**, the sulfur content estimated by elemental analysis is 305 µmol/g_{CNC}. The surface charge density is approximately 0.46 e/nm², as calculated using TEM and EA data.

Figure 5 presents TEM images of negatively stained CNC (**Figure 5a** and **5d**), CNCs decorated with $Pnipam_{2500}$ under LCST condition (**Figure 5b** and **5e**) and CNC-g-$Pnipam_{2500}$ after LCST (**Figure 5c** and **5f**). By comparison between **Figure 5d** and **Figure 5e**, the morphology of the rod-like particles is unchanged after peptidic grafting. Under LCST, $Pnipam_{2500}$ grafted CNCs seems to be well-dispersed. The individualization of nanocrystals can be attributed to the presence of polymer chains on the surface, which generate entropic repulsion forces between nanoparticles. Nonetheless, polymer chains are not visible on TEM images, due to their tiny size and a low surface density (hinder a detectable contrast in TEM stained grid). After LCST (**Figure 5c** and **5f**), CNC-g-$Pnipam_{2500}$ seems to be packed together and shows a 'bird-nest' configuration, due to the collapse $Pnipam_{2500}$ on the surface of TEMPO CNCs. These pictures are in agreement with $Pnipam_{2500}$ grafting and thermal aggregation of the system when the temperature is above the polymer LCST. Nonetheless, the system does not present CNC-g-$Pnipam_{2500}$ packed by 3-4 CNCs (as previously published by Azzam et al. (Azzam et al., 2016)) but a huge aggregate without well-defined size.

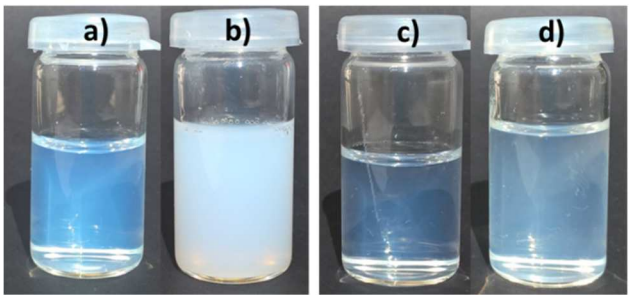

Figure 6: *Pictures of cellulose nanocrystals suspension: a) oxidized CNC without salt, b) TEMPO CNCs with 1M NaCl, c) CNC-g-$Pnipam_{2500}$ without salt and d) CNC-g-$Pnipam_{2500}$ with 1M NaCl. Each suspension has a concentration of 2 wt.%.*

An interesting property acquired by the presence of polymer chains (adsorbed or grafted) on the CNC surface is the colloidal stability with presence of electrolyte. **Figure 6** shows the behavior of TEMPO CNCs and polymer grafted CNCs when NaCl is added. Colloidal suspension of TEMPO CNCs (**Figure 6a**) immediately precipitates after addition of 1 M NaCl and forms a turbid suspension (**Figure 6b**). At the opposite, $Pnipam_{2500}$ grafted on CNCs suspension (**Figure 6c**) prevent any precipitation and remain stable the suspension in

presence of electrolyte (**Figure 6d**). Steric stabilization caused by the presence of polymer (grafted or adsorbed) was already reported in literature (Araki et al., 2001; Azzam et al., 2010; Kloser and Gray, 2010).

Figure 7 presents the rheological behavior of CNC-g-Pnipam$_{2500}$ and TEMPO CNCs + Pnipam$_{2500}$ under and above the PNIPAM LCST. System concentrations are 6.1 wt.% (estimated ratio is 25% of CNCs and 75% of Pnipam$_{2500}$). For grafted polymer (**Figure 7a**) the viscosity increases from 0.008 to 40 Pa·s at low shear rate when the LCST is reached. Nonetheless, in the case of polymer adsorption exclusively (**Figure 7b**), the viscosity increases only from 0.002 to 0.3 Pa·s when the LCST is reached. This observation shows a difference in kinetics of aggregation whereas similar amount of polymer is present. This confirms once again indirectly that there is a difference between these two CNCs materials.

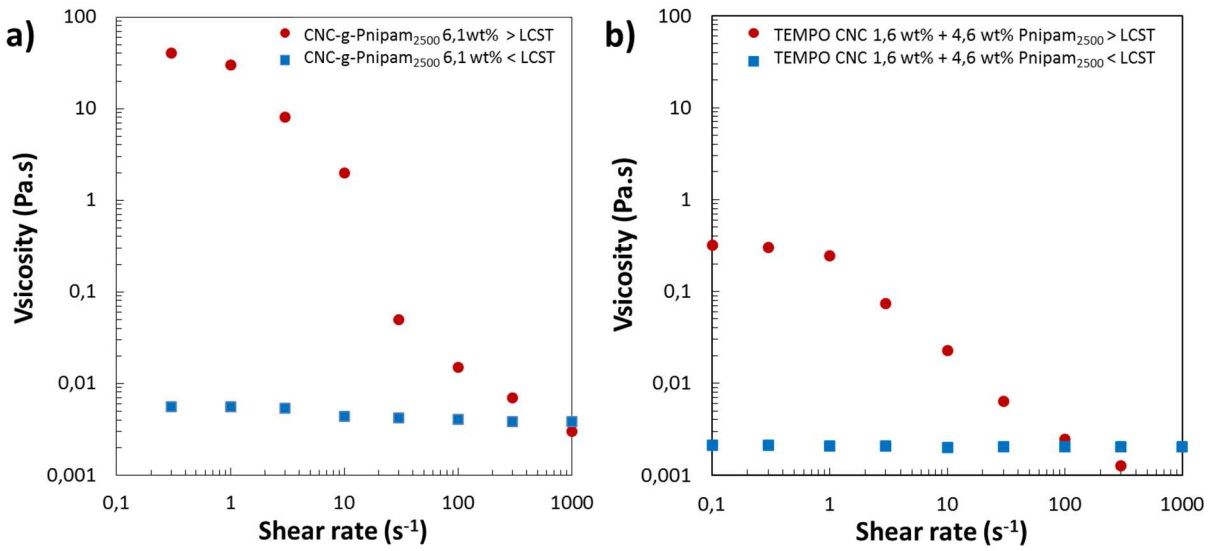

***Figure 7**: flow curves of a) CNC-g-Pnipam$_{2500}$ at 6.1 wt.% and b) TEMPO CNCs at 1.6 wt.% + Pnipam$_{2500}$ at 4.6 wt.% (final concentration 6.2 wt.%). Each graph presents the system flow curve under (blue square) and above (red dot) the PNIPAM LCST.*

This peptidic grafting is promising and can modify CNCs suspension properties by using water based grafting or adsorption. One drawback could be attributed to the low quantity of grafting (similar to adsorption) and to the time duration of such treatment.

4. Conclusions

In this study, thermo-sensitive $Pnipam_{2500}$ were successfully adsorbed and grafted (or both) onto oxidized cellulose nanocrystals by a green peptidic coupling. Results demonstrate the presence and the formation of the polymer onto the nanocrystals after multiple washings. The polymer density was sufficient to create a steric stabilization of the CNC-g-$Pnipam_{2500}$ in high ionic strength which prevents the flocculation. In spite of several methods, it has been difficult to distinguish the adsorbed from the grafted CNCs. However indirect methods show clearly a difference between the two samples indicating that of CNC-g-$Pnipam_{2500}$ has at least one part which is grafted. Thanks to this sufficient density, the thermo-reversible behavior of the polymer allows us to realize a thermo-reversible suspension composed with nanoparticles, CNCs, and biocompatible polymers, $Pnipam_{2500}$. CNCs give percolation network properties to the system and the polymer, a thermosensitive behavior, observed in rheology measurement. These results open the road to biomedical applications such as injectable hydrogel for reparative surgery and esthetic surgery.

5. Acknowledgment

This work has been partially supported by the PolyNat Carnot Institute (Investissements d'Avenir - grant agreement n°ANR-16-CARN-0025-01). This research has been possible thanks to the facilities of the TekLiCell platform funded by the Région Rhône-Alpes (ERDF: European regional development fund). LGP2 is part of the LabEx Tec 21 (Investissements d'Avenir - grant agreement n°ANR-11-LABX-0030) and CDP Glyco@alps (Initiative d'excellence – grant agreement ANR-15-IDEX02). We would like to thank Jean-Luc PUTEAU (Univ. Grenoble Alpes, CNRS, CERMAV, FRANCE) for his expertise in providing TEM imaging. The authors thank the NanoBio-ICMG platform (Grenoble, FR 2607) for granting access to the electron microscopy facility.

References

Alosmanov, R., Wolski, K., and Zapotoczny, S. (2017). Grafting of thermosensitive poly(N-isopropylacrylamide) from wet bacterial cellulose sheets to improve its swelling-drying ability. Cellulose *24*, 285–293.

Araki, J., Wada, M., and Kuga, S. (2001). Steric Stabilization of a Cellulose Microcrystal Suspension by Poly(ethylene glycol) Grafting. Langmuir *17*, 21–27.

Atalla, R.H., and VanderHart, D.L. (1999). The role of solid state 13C NMR spectroscopy in studies of the nature of native celluloses. Solid State Nucl. Magn. Reson. *15*, 1–19.

Azzam, F., Heux, L., Putaux, J.-L., and Jean, B. (2010). Preparation By Grafting Onto, Characterization, and Properties of Thermally Responsive Polymer-Decorated Cellulose Nanocrystals. Biomacromolecules *11*, 3652–3659.

Azzam, F., Siqueira, E., Fort, S., Hassaini, R., Pignon, F., Travelet, C., Putaux, J.-L., and Jean, B. (2016). Tunable Aggregation and Gelation of Thermoresponsive Suspensions of Polymer-Grafted Cellulose Nanocrystals. Biomacromolecules *17*, 2112–2119.

Bulpitt, P., and Aeschlimann, D. (1999). New strategy for chemical modification of hyaluronic acid: Preparation of functionalized derivatives and their use in the formation of novel biocompatible hydrogels. J. Biomed. Mater. Res. *47*, 152–169.

Camarero Espinosa, S., Rothen-Rutishauser, B., Johan Foster, E., and Weder, C. (2016). Articular cartilage: from formation to tissue engineering. Biomater. Sci. *4*, 734–767.

Cao, Y., Zhang, C., Shen, W., Cheng, Z., Yu, L. (Lucy), and Ping, Q. (2007). Poly(N-isopropylacrylamide)–chitosan as thermosensitive in situ gel-forming system for ocular drug delivery. J. Controlled Release *120*, 186–194.

Chauve, G., and Bras, J. (2014). Industrial point of view of nanocellulose materials and their possible applications. Handb. Green Mater. World Sci. 233–252.

Chen, X., Huang, L., Sun, H.-J., Cheng, S.Z.D., Zhu, M., and Yang, G. (2014). Stimuli-Responsive Nanocomposite: Potential Injectable Embolization Agent. Macromol. Rapid Commun. *35*, 579–584.

Cho, J.H., Kim, S.-H., Park, K.D., Jung, M.C., Yang, W.I., Han, S.W., Noh, J.Y., and Lee, J.W. (2004). Chondrogenic differentiation of human mesenchymal stem cells using a thermosensitive poly(N-isopropylacrylamide) and water-soluble chitosan copolymer. Biomaterials *25*, 5743–5751.

Da Silva Perez, D., Montanari, S., and Vignon, M.R. (2003). TEMPO-Mediated Oxidation of Cellulose III. Biomacromolecules *4*, 1417–1425.

Das, D., Ghosh, P., Ghosh, A., Haldar, C., Dhara, S., Panda, A.B., and Pal, S. (2015). Stimulus-Responsive, Biodegradable, Biocompatible, Covalently Cross-Linked Hydrogel Based on

576 Dextrin and Poly(N-isopropylacrylamide) for in Vitro/in Vivo Controlled Drug Release. ACS
577 Appl. Mater. Interfaces *7*, 14338–14351.

578 De France, K.J., Chan, K.J.W., Cranston, E.D., and Hoare, T. (2016). Enhanced Mechanical
579 Properties in Cellulose Nanocrystal–Poly(oligoethylene glycol methacrylate) Injectable
580 Nanocomposite Hydrogels through Control of Physical and Chemical Cross-Linking.
581 Biomacromolecules *17*, 649–660.

582 De France, K.J., Hoare, T., and Cranston, E.D. (2017). Review of Hydrogels and Aerogels
583 Containing Nanocellulose. Chem. Mater. *29*, 4609–4631.

584 Domingues, R.M.A., Gomes, M.E., and Reis, R.L. (2014). The Potential of Cellulose
585 Nanocrystals in Tissue Engineering Strategies. Biomacromolecules *15*, 2327–2346.

586 Dong, S., and Roman, M. (2007). Fluorescently Labeled Cellulose Nanocrystals for Bioimaging
587 Applications. J. Am. Chem. Soc. *129*, 13810–13811.

588 Dufresne, A. (2013). Nanocellulose: a new ageless bionanomaterial. Mater. Today *16*, 220–
589 227.

590 Eichhorn, S.J., Dufresne, A., Aranguren, M., Marcovich, N.E., Capadona, J.R., Rowan, S.J.,
591 Weder, C., Thielemans, W., Roman, M., Renneckar, S., et al. (2010). Review: current
592 international research into cellulose nanofibres and nanocomposites. J. Mater. Sci. *45*, 1–33.

593 Endes, C., Camarero-Espinosa, S., Mueller, S., Foster, E.J., Petri-Fink, A., Rothen-Rutishauser,
594 B., Weder, C., and Clift, M.J.D. (2016). A critical review of the current knowledge regarding
595 the biological impact of nanocellulose. J. Nanobiotechnology *14*, 78.

596 Eyley, S., and Thielemans, W. (2014). Surface modification of cellulose nanocrystals.
597 Nanoscale *6*, 7764–7779.

598 Follain, N., Marais, M.-F., Montanari, S., and Vignon, M.R. (2010). Coupling onto surface
599 carboxylated cellulose nanocrystals. Polymer *51*, 5332–5344.

600 Fujishige, S., Kubota, K., and Ando, I. (1989). Phase transition of aqueous solutions of poly
601 (N-isopropylacrylamide) and poly (N-isopropylmethacrylamide). J. Phys. Chem. *93*, 3311–
602 3313.

603 Gicquel, E. (2017). Development of stimuli-responsive cellulose nanocrystals hydrogels for
604 smart applications. Ph.D. Thesis. Grenoble Alpes University.

605 Gicquel, E., Martin, C., Yanez, J.G., and Bras, J. (2017). Cellulose nanocrystals as new bio-
606 based coating layer for improving fiber-based mechanical and barrier properties. J. Mater.
607 Sci. *52*, 3048–3061.

608 Habibi, Y. (2014). Key advances in the chemical modification of nanocelluloses. Chem. Soc.
609 Rev. *43*, 1519–1542.

610 Habibi, Y., Chanzy, H., and Vignon, M.R. (2006). TEMPO-mediated surface oxidation of
611 cellulose whiskers. Cellulose *13*, 679–687.

612 Habibi, Y., Lucia, L.A., and Rojas, O.J. (2010). Cellulose Nanocrystals: Chemistry, Self-
613 Assembly, and Applications. Chem. Rev. *110*, 3479–3500.

614 Hebeish, A., Farag, S., Sharaf, S., and Shaheen, T.I. (2014). Thermal responsive hydrogels
615 based on semi interpenetrating network of poly(NIPAm) and cellulose nanowhiskers.
616 Carbohydr. Polym. *102*, 159–166.

617 Hemraz, U.D., Lu, A., Sunasee, R., and Boluk, Y. (2014). Structure of poly(N-
618 isopropylacrylamide) brushes and steric stability of their grafted cellulose nanocrystal
619 dispersions. J. Colloid Interface Sci. *430*, 157–165.

620 Hoeng, F., Denneulin, A., and Bras, J. (2016). Use of nanocellulose in printed electronics: a
621 review. Nanoscale *8*, 13131–13154.

622 Isogai, A., Saito, T., and Fukuzumi, H. (2011). TEMPO-oxidized cellulose nanofibers.
623 Nanoscale *3*, 71–85.

624 Jorfi, M., and Foster, E.J. (2015). Recent advances in nanocellulose for biomedical
625 applications. J. Appl. Polym. Sci. *132*.

626 Kan, K.H.M., Li, J., Wijesekera, K., and Cranston, E.D. (2013). Polymer-Grafted Cellulose
627 Nanocrystals as pH-Responsive Reversible Flocculants. Biomacromolecules *14*, 3130–3139.

628 Klemm, D., Kramer, F., Moritz, S., Lindström, T., Ankerfors, M., Gray, D., and Dorris, A.
629 (2011). Nanocelluloses: A New Family of Nature-Based Materials. Angew. Chem. Int. Ed. *50*,
630 5438–5466.

631 Kloser, E., and Gray, D.G. (2010). Surface Grafting of Cellulose Nanocrystals with
632 Poly(ethylene oxide) in Aqueous Media. Langmuir *26*, 13450–13456.

633 Kubota, K., Fujishige, S., and Ando, I. (1990). Solution properties of poly (N-
634 isopropylacrylamide) in water. Polym J *22*, 15–20.

635 Lai, H., Chen, Q., and Wu, P. (2013). The core–shell structure of PNIPAM collapsed chain
636 conformation induces a bimodal transition on cooling. Soft Matter *9*, 3985.

637 Lanzalaco, S., and Armelin, E. (2017). Poly(N-isopropylacrylamide) and Copolymers: A Review
638 on Recent Progresses in Biomedical Applications. Gels *3*, 36.

639 Li, F., Biagioni, P., Bollani, M., Maccagnan, A., and Piergiovanni, L. (2013). Multi-functional
640 coating of cellulose nanocrystals for flexible packaging applications. Cellulose *20*, 2491–
641 2504.

642 Lima, L.H., Morales, Y., and Cabral, T. (2016). Ocular Biocompatibility of Poly-N-
643 Isopropylacrylamide (pNIPAM). J. Ophthalmol.

644 Lin, N., and Dufresne, A. (2014). Nanocellulose in biomedicine: current status and future
645 prospect. Eur. Polym. J. *59*, 302–325.

Lin, J.B., Isenberg, B.C., Shen, Y., Schorsch, K., Sazonova, O.V., and Wong, J.Y. (2012). Thermo-responsive poly(N-isopropylacrylamide) grafted onto microtextured poly(dimethylsiloxane) for aligned cell sheet engineering. Colloids Surf. B Biointerfaces *99*, 108–115.

Mangalam, A.P., Simonsen, J., and Benight, A.S. (2009). Cellulose/DNA Hybrid Nanomaterials. Biomacromolecules *10*, 497–504.

Missoum, K., Bras, J., and Belgacem, M.N. (2012). Organization of aliphatic chains grafted on nanofibrillated cellulose and influence on final properties. Cellulose *19*, 1957–1973.

Montanari, S., Rountani, M., Heux, L., and Vignon, M.R. (2005). Topochemistry of carboxylated cellulose nanocrystals resulting from TEMPO-mediated oxidation. Macromolecules *38*, 1665–1671.

Moon, R.J., Martini, A., Nairn, J., Simonsen, J., and Youngblood, J. (2011). Cellulose nanomaterials review: structure, properties and nanocomposites. Chem. Soc. Rev. *40*, 3941.

Naseri, N., Deepa, B., Mathew, A.P., Oksman, K., and Girandon, L. (2016). Nanocellulose-Based Interpenetrating Polymer Network (IPN) Hydrogels for Cartilage Applications. Biomacromolecules *17*, 3714–3723.

Ohya, S., Nakayama, Y., and Matsuda, T. (2004). In vivo evaluation of poly(N-isopropylacrylamide) (PNIPAM)-grafted gelatin as an in situ-formable scaffold. J. Artif. Organs *7*, 181–186.

Okahata, Y., Noguchi, H., and Seki, T. (1986). Thermoselective permeation from a polymer-grafted capsule membrane. Macromolecules *19*, 493–494.

Oksman, K., Mathew, A.P., Bismarck, A., Rojas, O., and Sain, M. (2014). Handbook of Green Materials: Processing Technologies, Properties and Applications: Volume 5 (World Scientific).

Pelton, R. (2010). Poly(N-isopropylacrylamide) (PNIPAM) is never hydrophobic. J. Colloid Interface Sci. *348*, 673–674.

Plunkett, K.N., Zhu, X., Moore, J.S., and Leckband, D.E. (2006). PNIPAM Chain Collapse Depends on the Molecular Weight and Grafting Density. Langmuir *22*, 4259–4266.

Rånby, B.G. (1951). Fibrous macromolecular systems. Cellulose and muscle. The colloidal properties of cellulose micelles. Discuss. Faraday Soc. *11*, 158–164.

Revol, J.-F., Bradford, H., Giasson, J., Marchessault, R.H., and Gray, D.G. (1992). Helicoidal self-ordering of cellulose microfibrils in aqueous suspension. Int. J. Biol. Macromol. *14*, 170–172.

Schild, H.G. (1992). Poly(N-isopropylacrylamide): experiment, theory and application. Prog. Polym. Sci. *17*, 163–249.

Senff, H., and Richtering, W. (1999). Temperature sensitive microgel suspensions: Colloidal phase behavior and rheology of soft spheres. J. Chem. Phys. *111*, 1705–1711.

682 Siqueira, G., Bras, J., and Dufresne, A. (2010a). Cellulosic Bionanocomposites: A Review of
683 Preparation, Properties and Applications. Polymers *2*, 728–765.

684 Siqueira, G., Bras, J., and Dufresne, A. (2010b). New Process of Chemical Grafting of Cellulose
685 Nanoparticles with a Long Chain Isocyanate. Langmuir *26*, 402–411.

686 Tang, J., Sisler, J., Grishkewich, N., and Tam, K.C. (2017). Functionalization of cellulose
687 nanocrystals for advanced applications. J. Colloid Interface Sci. *494*, 397–409.

688 Wang, X., and Wu, C. (1999). Light-Scattering Study of Coil-to-Globule Transition of a Poly(N-
689 isopropylacrylamide) Chain in Deuterated Water. Macromolecules *32*, 4299–4301.

690 Wu, C. (1998). Globule-to-Coil Transition of a Single Homopolymer Chain in Solution. Phys.
691 Rev. Lett. *80*, 4092–4094.

692 Wu, W., Huang, F., Pan, S., Mu, W., Meng, X., Yang, H., Xu, Z., Ragauskas, A.J., and Deng, Y.
693 (2015). Thermo-responsive and fluorescent cellulose nanocrystals grafted with polymer
694 brushes. J. Mater. Chem. A *3*, 1995–2005.

695 Zoppe, J.O., Habibi, Y., Rojas, O.J., Venditti, R.A., Johansson, L.-S., Efimenko, K., Österberg,
696 M., and Laine, J. (2010). Poly(N-isopropylacrylamide) Brushes Grafted from Cellulose
697 Nanocrystals via Surface-Initiated Single-Electron Transfer Living Radical Polymerization.
698 Biomacromolecules *11*, 2683–2691.

699 Zoppe, J.O., Österberg, M., Venditti, R.A., Laine, J., and Rojas, O.J. (2011). Surface Interaction
700 Forces of Cellulose Nanocrystals Grafted with Thermoresponsive Polymer Brushes.
701 Biomacromolecules *12*, 2788–2796.

702 Zubik, K., Singhsa, P., Wang, Y., Manuspiya, H., and Narain, R. (2017). Thermo-Responsive
703 Poly(N-Isopropylacrylamide)-Cellulose Nanocrystals Hybrid Hydrogels for Wound Dressing.
704 Polymers *9*, 119.

705